Soft Matter

Accepted Manuscript

ROYAL SOCIETY OF CHEMISTRY

www.rsc.org/softmatter

Soft Matter

ARTICLE

Effects of Excluded Volume and Hydrodynamic Interaction on the Deformation, Orientation and Motion of Ring Polymers in Shear Flow

Received 00th January 20xx,
Accepted 00th January 20xx

DOI: 10.1039/x0xx00000x
www.rsc.org/

Wenduo Chen,[a,b] Hongchao Zhao,[c] Lijun Liu,[b] Jizhong Chen,[b†] Yunqi Li,[a†] and Lijia An[b]

Ring polymer is a classical model to explore the behaviors of biomacromolecules. Compared with its linear counterpart in shear flow, the ring polymer should be more sensitive to excluded volume and hydrodynamic interaction attributed to the absence of chain ends. We carried out multiparticle collision dynamics combined with molecular dynamics simulation to study the effects of excluded volume and hydrodynamic interaction on the behaviors of ring polymers in shear flow. The results show that in the absence of the strong excluded volume interaction, the ring polymer prefers a two-strand linear conformation with high deformation and orientation in the flow-gradient plane, and the tank-treading motion is nearly negligible. Ring polymers without excluded volume show no significant difference to linear polymers in the scaling exponents for the deformation, orientation and tumbling motion. We also observed that the hydrodynamic interaction can efficiently slow down the relaxation of ring polymers while the scaling exponents against Weissenberg number have rarely been affected.

I. INTRODUCTION

Excluded volume (EV) and hydrodynamic interaction (HI) have been widely recognized as elementary physical components in the understanding of conformational and dynamical behaviors of linear polymers in dilute solutions[1, 2]. Ring polymer is one of the classical models for many biological macromolecules, such as plasmid, mitochondrial DNA, cyclic peptides and polysaccharides[3-8]. Compared with linear polymers, ring polymers have no end-groups and slightly higher monomer density, which normally lead to smaller size and faster self-diffusion[3]. Indeed, in good solvents, the presence of EV interaction makes ring polymers swell more and slows down the diffusion, while HI interaction facilitates chain diffusion[9]. A clear view of the effects of EV and HI on the deformation, orientation and motion of ring polymers in shear flow is still absent. A deep insight into the effects of EV and HI on ring polymers in shear flow is urgently needed to provide a thorough view from polymer physics for many biological processes, such as the manufacture of plasmid DNA[5], the segregation of the cyclic genome from bacteria[6], the migration of a cyclic DNA in a nanochannel[10, 11] and the ejection of viral DNA into the host[7], etc.

The EV effect is the tendency to repel any two beads from close packing[1, 2]. The influence of EV on the behaviors of polymer chains in shear flow is a subject of great interest including the fundamental understanding of solvent quality[1], and novel technological applications for polymer separation and purification[12, 13]. Experimental measurements and numerical computations have revealed a number of consequences contributed from the EV for linear polymers in shear flow[14-21]. Experimentally, Muller et al. observed that linear polymers have larger stretching and weaker orientation in good solvents than in theta solvents based on a light scattering study of in-situ flow[14, 21]. Springer *et al.* also found that the alignment of polystyrene chains along the flow direction becomes weaker in good solvents through a wide-angle laser light scattering[15]. Numerically, Muthukumar *et al.* found that linear polymers expand more relative to their quiescent state in theta solvents than in good solvents at low shear rates ($\dot{\gamma}$), and the stretching of polymer chains is much smaller than the prediction by Rouse or Zimm model via Brownian dynamics (BD) simulation[19]. Prakash *et al.* found that the EV interaction can suppress the orientation of the polymers along the flow direction[20]. Furthermore, Larson *et al.* found the scaling exponent of tumbling (TB) frequency against Peclet number of linear polymers is 2/3 in the presence of HI, unaffected by the EV interaction[23,24]. For ring polymers, the close topology results in higher monomer density, and EV interaction shows stronger impact[22-26]. According to recent studies, ring polymer has one more tank-treading (TT) motion over the common TB motion of linear polymer to relax the strain from shear flow[27-30]. How the EV interaction affects these two motions and the

[a] *Key Laboratory of Synthetic Rubber & Laboratory of Advanced Power Sources, Changchun Institute of Applied Chemistry, Chinese Academy of Sciences, 5625 Renmin Street, Changchun, PR China, 130022.*
[b] *State Key Laboratory of Polymer Physics and Chemistry, Changchun Institute of Applied Chemistry, Chinese Academy of Sciences, 5625 Renmin Street, Changchun, PR China, 130022.*
[c] *Changchun Institute of Optics, Fine Mechanics and Physics, Chinese Academy of Sciences, 3888 Dong Nanhu Road, Changchun, PR China, 130033.*
† Author to whom correspondence should be addressed. Electronic mail: jzchen@ciac.ac.cn & yunqi@ciac.ac.cn.
Electronic Supplementary Information (ESI) available:
See DOI: 10.1039/x0xx00000x

conformation change for ring polymers in shear flow still has not been reported yet.

On the other hand, the consideration of HI can greatly facilitate the understanding of motions of polymers in solutions[1]. For example, Rouse model neglects HI and the relaxation time scale against polymer chain length is $\tau \sim N^{1+2\nu}$ with ν equals 0.5 for theta solvents and 0.59 for good solvents, while Zimm model considering HI provides $\tau \sim N^{3\nu}$ and the latter agrees with the experimental measurements well[1,2]. The HI makes buried or exposed polymer monomers feel different solvent drag[31]. In the coiled state, interior monomers are shielded from the full solvent velocity by outer portions of the polymer chain. In the fully extended conformation, more monomers are exposed to the flow, and the effects of HI are diminished[31]. Several recent studies have revealed the impacts of HI on the deformation, orientation and motion of linear polymers in shear flow[17,19,31-33]. Sendner and Netz found that the dominant HI, which screens interior monomers from hydrodynamic drag, can reduce the stretching of linear chains under shear[17]. By means of BD simulation, Jendrejack *et al.* found the conformation, motion and the average steady-state elongation scaled with Weissenberg number ($Wi=\dot{\gamma}\tau$ with $\dot{\gamma}$ is shear rate and τ is the longest relaxation time, respectively) of λ-phage DNA can be predicted by either free-draining or HI mode[32]. Further, Chu *et al.* also found consistency in the stretching, orientation and TB motion of single DNA by both BD simulation and single-molecule fluorescence microscopy[31, 33]. It is interesting that normalized with *Wi*, the differences in deformation, orientation and dimensionless frequency in TB motion are almost undetected in the presence or absence of HI[31-33]. Statement on the HI effect on the conformation, orientation and motion of linear polymers to relax strain in shear flow is quite clear, but for ring polymers, it is still poorly understood.

Directly illustrate the effects of EV and HI on the deformation, orientation and motion of ring polymers is still full of challenges for theoretical analyses (unique topology and too complicate) and experimental approaches (too sensitive to component impurity and environmental fluctuations). Alternatively, computer simulation is fairly suitable for such challenge and bridges theoretical models with experimental observations[34, 35]. Therefore, we applied a hybrid multi-particle collision dynamics (MPCD) and Molecular Dynamics (MD) simulation to study the effects of EV and HI on conformational and dynamical properties of ring polymers in shear flow[36, 37]. The outline of this work is organized as follows: In section II we give a brief description of MPCD-MD simulation method and settings. In section III we present the effects of EV and HI on the deformation, orientation and motion of ring polymers in simple shear flow. Finally, the principal conclusions of this work are summarized.

II. MODEL AND SIMULATION METHOD

We employ a hybrid simulation method, which combines standard molecular dynamics (MD) simulation for the flexible ring polymers with MPCD simulation for explicit solvent particles[38-43]. The ring polymer chains consist of N beads of mass M each. The consecutive beads are connected by a bead-spring model and the bond potential U_b follows Hooke's law[44, 45],

$$U_b = \frac{k}{2}\sum_{i=1}^{N-1}(r - r_0)^2 \tag{1}$$

Here r_0 is the equilibrium bond length and k is the spring constant.

The non-bonded interactions use a truncated and shifted Lennard-Jones potential to model the EV among polymer beads,

$$U_{EV} = \begin{cases} 4\varepsilon[(\frac{\sigma}{r})^{12} - (\frac{\sigma}{r})^{6}] + \varepsilon & r \le r_{cut} \\ 0 & r > r_{cut} \end{cases} \tag{2}$$

where $r=|\mathbf{r}_i-\mathbf{r}_j|$ denotes the distance between beads i and j located at $\mathbf{r}_i$ and $\mathbf{r}_j$. ε and σ are taken as the units of energy and length, respectively. The short-range, purely repulsive interaction is taken into account by choosing r_{cut} at $2^{1/6}\sigma$. The dynamics of solute particles are determined by Newton's equation of motion, which is integrated by the velocity Verlet algorithm with the time step h_p.

In order to make full treatment of hydrodynamic effects for polymer solutions, the explicit solvent is described by MPCD approach[36, 37]. Solvent is modelled of N_{st} point-like particles of mass m, which interact with each other by a stochastic process. In the streaming step, the solvent particles propagates ballistically and their positions are updated according to[46]

$$\mathbf{r}_i(t+h) = \mathbf{r}_i(t) + h\mathbf{v}_i(t) \tag{3}$$

where $i = 1,\ldots, N_{st}$ and h is the time interval between collisions. In the collision step, the particles are sorted into cubic cells with length a, and their relative velocities, with respect to the centre-of-mass velocity of each cell $\mathbf{v}_{cm}(t)$, are rotated by an angle φ around a random axis $\mathbf{R}(\varphi)$ [36], i.e.

$$\mathbf{v}_i(t+h) = \mathbf{v}_{cm}(t) + \mathbf{R}(\varphi)[\mathbf{v}_i(t) - \mathbf{v}_{cm}(t)] \tag{4}$$

where $\mathbf{v}_i(t)$ is the velocity of particle i at time t and the centre-of-mass velocity

$$\mathbf{v}_{cm}(t) = \frac{1}{N_{st}^c}\sum_{j=1}^{N_{st}^c}\mathbf{v}_j(t) \tag{5}$$

N_{st}^c is the total number of solvent particles within the collision cell.

Polymer has no interaction with solvent except the collision step in MPCD simulation, and the centre-of-mass velocities are[33,34]

$$\mathbf{v}_{cm}(t) = \frac{\sum_{i=1}^{N_{st}^c} m\mathbf{v}_i(t) + \sum_{j=1}^{N_{se}^c} M\mathbf{v}_j(t)}{mN_{st}^c + MN_{se}^c} \tag{6}$$

where N_{se}^c is the number of solute particles in the collision cell. A random-shift procedure is applied before each collision step to restore Galilean invariance[47]. Mass, momentum, and energy are conserved in the collisions, leading to the buildup of correlations between the particles and giving rise to HI.

A standard procedure to evaluate HI is to tackle the same problem by simulations with (+HI) and without HI (-HI). The basic idea for switching HI is to randomly interchange velocities of all solvent particles after each collision step[48]. In this process, local conservation laws are violated but the total momentum and energy are conserved. An efficient method is that each solute particle is coupled with an effective solvent momentum **P** which is directly chosen from a Maxwell-Boltzmann distribution of variance $m\rho k_B T$ and a mean given by the average momentum of the fluid field. Here,

T is the temperature, k_B the Boltzmann constant and ρ the average number of solvent particles per collision cell. The total centre-of-mass velocity, which is used in the collision step, is then given by

$$\mathbf{v}_{cm}(t) = \frac{M\mathbf{v}+\mathbf{P}}{m\rho+M} \quad (7)$$

The solute trajectory is then determined using MD, and the interaction with the solvent is performed in every collision step.

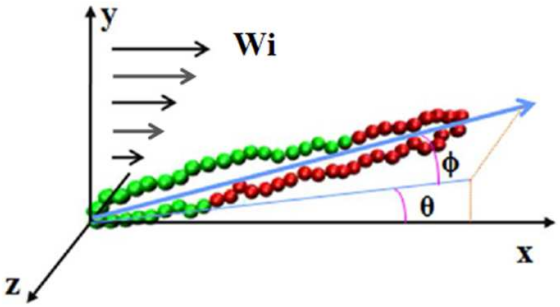

FIG. 1. Sketch of an individual ring polymer in simple shear flow. ϕ is the angle between the principal vector and its projection onto the flow-gradient plane and θ is the angle between this projection and the flow direction. The monomers are colored red and green for clarity.

To achieve the simple shear flow, we apply Lees-Edwards boundary condition[49], as shown in Fig.1. The velocity field is given by

$$v_x = \dot{\gamma}y, v_y = 0, v_z = 0 \quad (8)$$

All simulations are performed in NVT assemble and a local Maxwellian thermostat is used to maintain a constant temperature T. MPCD with the rotation angle φ=130°, σ=a=1.0, ε=1.0, k_BT/ε=1.0, where k_B is the Boltzmann constant. The collision time h=0.1τ_p, MD time step h_p=0.0005τ_p, with $\tau_p=\sqrt{ma^2/(k_BT)}$. Small collision time h and large rotation angle φ are used to obtain large Schmidt numbers required for fluid-like behaviors[46]. The average number of solvent particles per collision cell ρ=10, M=ρm and m=1.0. The viscosity of solvent fluid is 8.7$(\varepsilon m)^{1/2}/\sigma^2$. The equilibrium bond length r_0=0.97σ and the spring constant k=10000ε/σ^2. The large spring constant k ensures that the small fluctuation of the equilibrium bond length. The chain lengths N are changing from 10 to 120 in static solution conditions, and accordingly the system sizes change from 15a × 15a × 15a to 60a × 60a × 60a. In simple shear flow, the considered chain length N is 60, and accordingly the system size is 60a × 40a × 40a.

III. RESULTS AND DISCUSSION

A.Scaling behaviors of equilibrium properties

Before the presentation of ring polymers in shear flow, the roles of EV and HI on the conformation and the relaxation of ring polymers are studied. Fig.2 shows the scaling relationship of the mean-square radius of gyration $\langle R_g^2\rangle$ (here $\langle\rangle$ denotes ensemble average) and the longest relaxation time τ with various polymer lengths, ranging from N = 10 to N = 120. The theory predicts that the size of polymer satisfies a scaling relationship of $\langle R_g^2\rangle \sim N^{2\nu}$, with exponents $\nu \approx 0.59$, 0.50 for good solvents and theta solvents[1], respectively. In our simulation, the mean-square radius of gyration $\langle R_g^2\rangle$ of ring polymers yields an exponential relationship $\langle R_g^2\rangle \sim N^{1.22}$ with EV and $\langle R_g^2\rangle \sim N^{1.00}$ without EV (Table.1), in good agreement with theory prediction for the ideal and real chain models[1]. In addition, it is obvious that the chain size of a ring polymer with EV is larger than that without EV. It means that under the influence of EV interaction, the ring polymers swell more in good solvents than in theta solvents. The $\langle R_g^2\rangle$ with HI and without HI collapsing into a single master curve implies that the equilibrium chain conformation is not perturbed by HI.

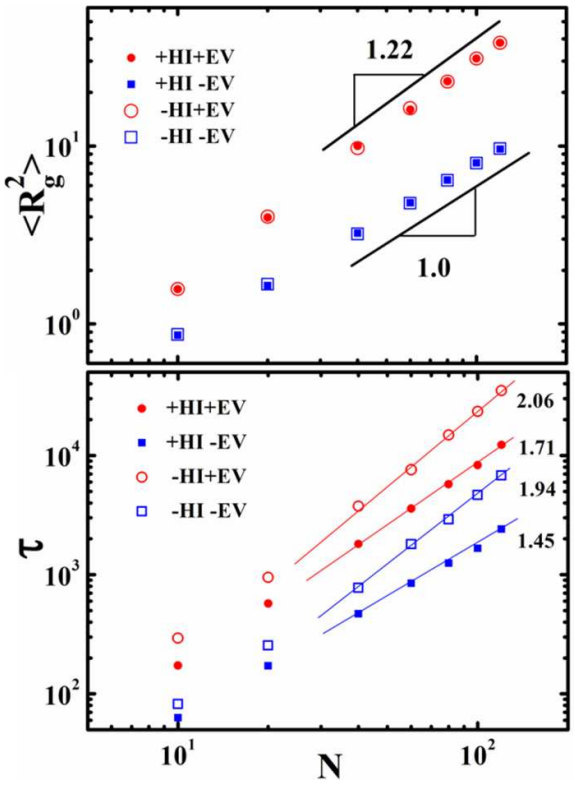

FIG. 2. The log-log plot of the mean-square radius of gyration $\langle R_g^2\rangle$ and the longest relaxation time τ as a function of chain lengths N varied from 10 to 120. The solid lines indicate the power law dependencies.

The dynamical properties of individual ring polymers in dilute polymer solutions at equilibrium state can be studied by the longest relaxation time τ[50]. The longest relaxation time τ for a ring polymer is determined based on the exponential decay of autocorrelation function of the diameter vector, which is defined as a vector joining two beads in the same chain that are separated by N/2 beads[50]. Fig.2(b) shows the relaxation time τ as a function of chain length for ring polymers in the presence and absence of EV and HI. The chain with smaller size diffuses faster, so the longest relaxation time τ increases with EV effects. Moreover, in the absence of HI, the motion of a bead does not affect other beads except through the spring force. With the dominant HI, the diffusion of one of the beads affects all the others through the flow of solvent. Thus, HI increases

the diffusivity of the chain, especially for a long chain, compared with a group of independently moving beads[1, 2]. For short chains such as the chain with $N=20$, the $\langle R_g^2 \rangle$ is 1.64 without EV, which is consitent with the theory for the ideal chain, $\langle R_g^2 \rangle = Nb^2/12$. Though it seems the radius is small, the HI is also pronounced because the Zimm model treats the pervaded volume of polymer chains as a solid object moving through the surrounding solvent. For long chains ($N \geq 40$), the longest relaxation times exist the chain length dependence with the power law $\tau \sim N^{\zeta}$. We find that for +HI+EV $\zeta = 1.71$, for -HI+EV $\zeta = 2.06$, for +HI-EV $\zeta = 1.45$ and for -HI-EV $\zeta = 1.94$ (Table.1). These exponents are slightly less than the prediction by Rouse and Zimm theories attributed to the absence of chain ends compared with linear polymers[51]. Here it is worth to note that both Rouse and Zimm theories are accurate for polymer chains with sufficiently long length. The chain length in this work is up to 120, and it should be an asymptotic scaling of the theoretical prediction.

Table 1. Scaling exponents for the mean-square radius of gyration and the longest relaxation time against chain length, influenced by EV and HI.

scaling	**ν**		**ζ**		
exponents	simulation	theory	simulation	Rouse	Zimm
+HI+EV	0.61	0.59	1.71	_	1.77
+HI-EV	0.50	0.50	1.45	_	1.50
-HI+EV	0.61	0.59	2.06	2.18	_
-HI -EV	0.50	0.50	1.94	2.00	_

B.Deformation of ring polymers in shear flow

We will now discuss the effects of EV and HI on the conformational properties of individual ring polymers in simple shear flow. The shear strength is characterized by the Weissenberg number. For small shear strengths ($Wi < 1$), the shapes of the elliptical polymer coils have no detectable changes compared with the equilibrium conformation. In the strong shear flow regime ($Wi > 1$), the ring chains have obvious deformations and they are not able to relax back to the equilibrium conformation. The characteristic value $Wi = 1$ plays an essential role in characterizing the microscopic deformational, orientational and dynamical properties of polymers in simple shear flow[52, 53].

The microscopic conformational properties of individual ring polymers can be conveniently quantified by gyration tensor $G_{\alpha\xi}$, which has direct influence on the macroscopic solution behavior in shear flow[45]. It is defined as

$$G_{\alpha\xi} = \frac{1}{N}\sum_{i=1}^{N} \Delta r_{i,\alpha} \Delta r_{i,\xi} \qquad (8)$$

where $\Delta r_{i,\alpha}$ is the distance between particle i and the centre-of-mass of the ring polymer, and $\alpha,\xi \in (x,y,z)$ denote Cartesian components. The diagonal components, $\langle G_{\alpha\alpha}(\dot{\gamma}) \rangle$, are the squared radii of gyration in α direction. In addition, the three eigenvalues of $G_{\alpha\xi}(\dot{\gamma})$ are denoted by the largest eigenvalue $G_1(\dot{\gamma})$, the middle $G_2(\dot{\gamma})$, and the smallest $G_3(\dot{\gamma})$, and their sum $\{\langle G_1(\dot{\gamma}) \rangle + \langle G_2(\dot{\gamma}) \rangle + \langle G_3(\dot{\gamma}) \rangle\}$ is just the mean-square radius of gyration $\langle R_g^2(\dot{\gamma}) \rangle$. In the absence of flow, the statistical conformation of a ring polymer is spherical, i.e., $\langle G_{xx}(0) \rangle = \langle G_{yy}(0) \rangle = \langle G_{zz}(0) \rangle = \langle R_g^2(0) \rangle / 3$[49].

Soft Matter

ARTICLE

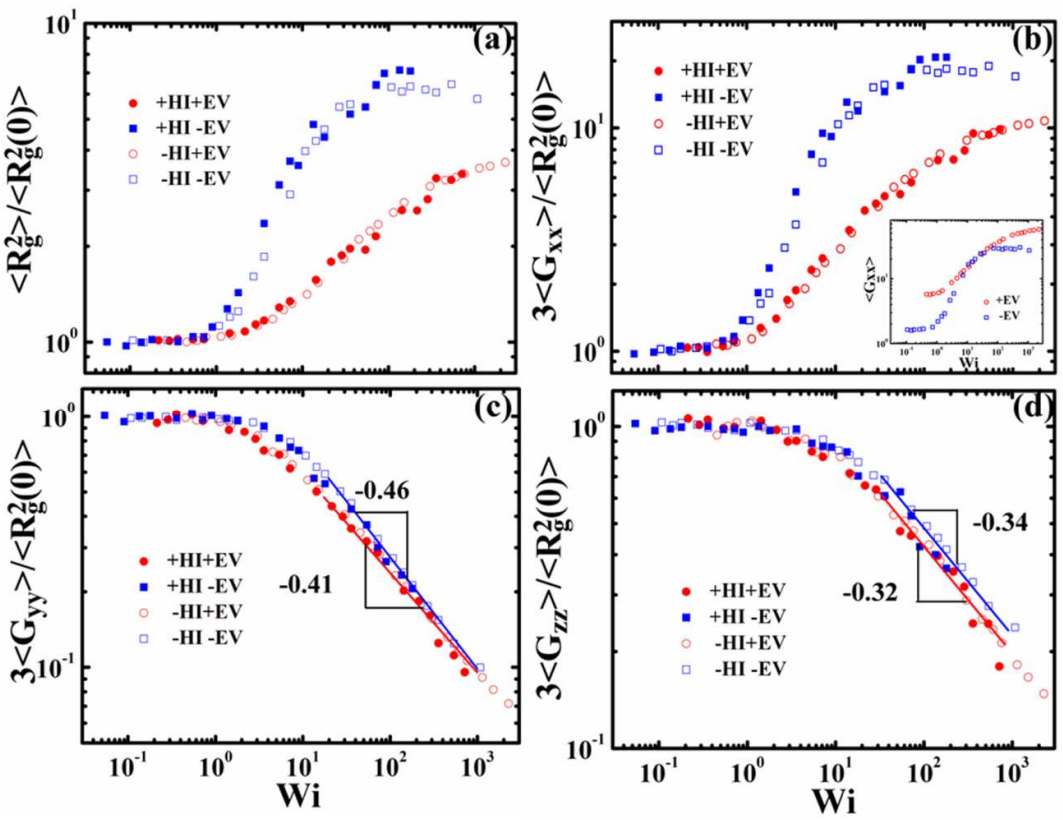

FIG. 3. (a) The mean-square radius of gyration normalized with the radius of gyration under equilibrium $\langle R_g^2 \rangle / \langle R_g^2(0) \rangle$ (b) the flow component $\langle G_{xx} \rangle / \langle R_g^2(0) \rangle$, (c) the gradient component $\langle G_{yy} \rangle / \langle R_g^2(0) \rangle$, and (d) the vorticity component $\langle G_{zz} \rangle / \langle R_g^2(0) \rangle$ as a function of the Weissenberg number for $N = 60$ with and without excluded volume (±EV) and hydrodynamic interaction (±HI). The solid lines in (c) and (d) are power law fits to the data.

Fig.3 displays three diagonal elements of the gyration tensor $\langle G_{\alpha\alpha} \rangle$ normalized to the equilibrium value $\langle R_g^2(0) \rangle$ as a function of *Wi* for ring polymers in the presence or absence of EV and HI. As shown in Fig.3(a) and (b) , for $Wi < 1$, $\langle R_g^2(0) \rangle$ remains practically unaffected by the applied flow, and $\langle G_{xx} \rangle$ is only weakly perturbed for all considered models. In this regime, ring polymers have no obvious deformation and only align along the flow direction. As *Wi* increases, the values of $\langle G_{xx} \rangle$ increase rapidly, implying that ring polymers not only orient in the flow direction but also assume a stretched conformation. At high Weissenberg numbers, a platform appears as a consequence of the finite chain extensibility which yields an average stretching smaller than half of the contour length[53, 54]. Since the small equilibrium size, the relative stretching $3\langle G_{xx} \rangle / \langle R_g^2(0) \rangle$ without EV is larger than the case with EV at the same *Wi*. Different asymptotic values are also assumed, consistent with the previous observation for linear polymers[52]. In fact, the absolute stretching of ring polymers with EV is slightly larger than the polymers without EV, as can be seen in the inset of Fig.3(b). In addition, scaled with *Wi*, the simulation points with/without HI almost fall on the same line. A similar elongation behavior was also observed for linear polymers in shear flow[32].

The ensemble-averaged gradient component of the average gyration tensor $\langle G_{yy} \rangle$ is of interest because this quantity describing the mean thickness of polymers is tightly linked with shear thinning in shear flow[52]. When shear strength is not large enough ($Wi < 1$), the value of $3\langle G_{yy} \rangle / \langle R_g^2(0) \rangle$ is about 1, reflecting the fact that the

deformation is undetectable, as shown in Fig.3(c). As *Wi* increases, the stretching of the ring polymers in the flow direction is accompanied by shrinking in the gradient and vorticity directions. Under the effect of EV interaction, the values of relative compression $3\langle G_{yy}\rangle/\langle R_g^2(0)\rangle$ decrease for a given *Wi*. In addition, a universal power law $\langle G_{yy}\rangle/\langle R_g^2(0)\rangle \sim Wi^{\mu}$ is obtained over the considered *Wi* range (*Wi* > 20). The scaling exponent μ=–0.41 for ring polymers with EV is larger than -0.46 without EV, which is similar to -0.45 for linear polymers in previous experiments and simulations[52, 55]. The qualitative difference between the decays with and without EV is attributed to the strong self-avoidance of ring polymers. In the absence of HI, individual ring polymers tend to form a two-strand linear conformation rather than an ellipse in the flow-gradient plane (see supporting information).

Fig.3(d) presents the ensemble-averaged vorticity component of the average gyration tensor $3\langle G_{zz}\rangle/\langle R_g^2(0)\rangle$. With *Wi* increasing, the values of $\langle G_{zz}\rangle$ drop significantly from a plateau value. For large *Wi*, the values of $\langle G_{zz}\rangle$ falling on the same curve with universal dependences, $\langle G_{zz}\rangle/\langle R_g^2(0)\rangle \sim Wi^{\mu}$, with μ=-0.32 in the presence of EV and μ=-0.34 in the absence of EV. It implies that the vorticity component of the average gyration tensor has no qualitative change under the effect of EV. In addition, simulation results of both with HI and without HI models show the similar values of $3\langle G_{zz}\rangle/\langle R_g^2(0)\rangle$ as a function of *Wi* (see Fig.3).

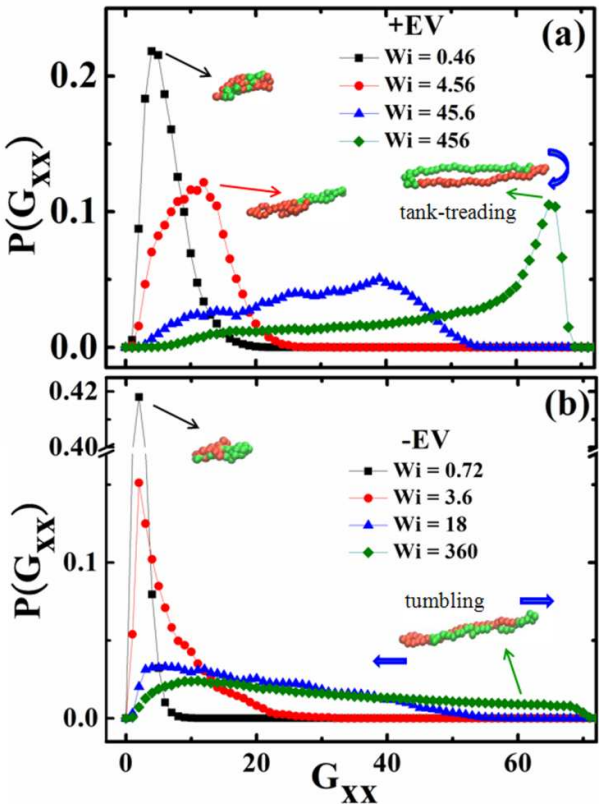

FIG. 4. The probability distribution functions of the flow-direction component $P(G_{xx})$ for various Weissenberg numbers with (a) and without (b) EV interactions.

In order to deeply understand the effects of EV and HI on the stretching behaviors of ring polymers, the probability distribution functions (PDFs) of the average molecular extension $P(G_{XX})$ are presented in Fig.4. For small *Wi* (*Wi* < 1), the distribution is practically Gaussian. The curve of $P(G_{XX})$ without EV has higher peaks and thinner width than the curve with EV, because the flexible ring polymer without self-avoidance has a smaller size. As shear strength increases, the $P(G_{XX})$ without EV manifests decaying peaks, the width of which grows considerably, and deviates from the Gaussian shape to a uniform shape. These curves are similar to the experimental and simulation results of the linear polymers[30,53]. The uniform shape is caused by an almost uniform speed of conformational changes for a given *Wi* in the TB motions. The rather interesting observation is that in the presence of EV the peaks decay first and then increase. It reflects that ring polymers undergo the TT motions, in which ring chains assume the continuous extension[27-30]. Without self-avoidance, individual ring polymers tend to form a two-strand line rather than an ellipse shape in the flow-gradient plane. Accordingly, TT motion is nearly negligible (see supporting information).

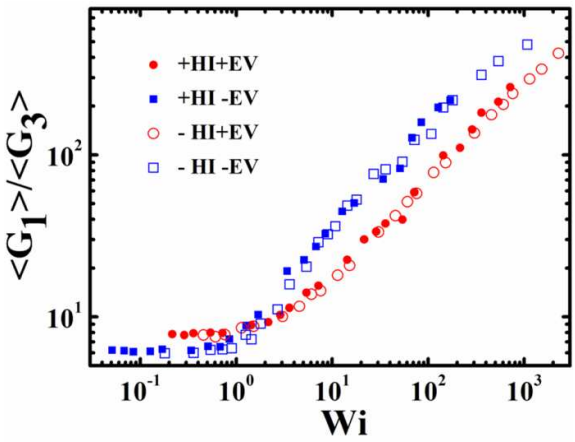

FIG. 5. Aspect ratio of the largest (G_1) and smallest (G_3) eigenvalues of the average gyration tensor as a function of the Weissenberg number.

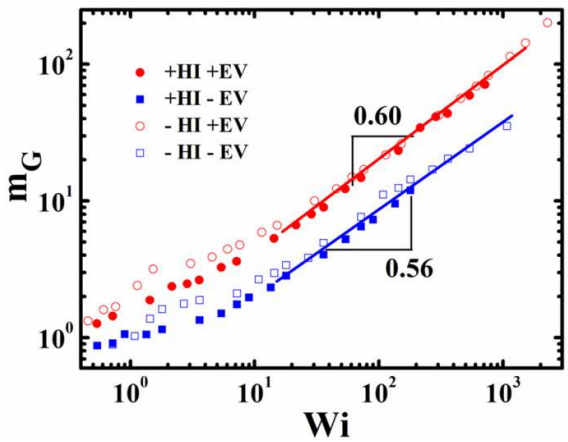

FIG. 6. Orientational resistance m_G for ring polymers in the presence or absence of EV and HI as a function of the Weissenberg number. The solid lines are power law fits to the data.

The three eigenvalues of the gyration tensor are also calculated in our simulations to fully identify the deformation of the shapes of ring polymers subjected to shear flow. The ratio $\langle G_1\rangle/\langle G_3\rangle$ denotes the asphericity of polymer chains, because if the value of $\langle G_1\rangle/\langle G_3\rangle$ equals to unity means that the distribution is spherical, while it diverges in the limit of a long rod[49]. Fig.5 shows the aspect ratios in the presence or absence of EV and HI. Considering the diagonal elements of the gyration tensor shown in Fig.3, the ratio $\langle G_1\rangle/\langle G_3\rangle$ is essentially constant at low shear strengths ($Wi < 1$) implies that the ring polymers are close to their equilibrium structure. With Wi increasing, the shape of a ring polymer without EV assumes a longer rod than the case with EV. It confirms the fact that the stretched ring polymers without EV prefer to form a two-strand line. Furthermore, normalized with Wi, the simulation results reveal that the effects of HI is almost undetected in the conformational properties of ring polymers.

C.Orientation of ring polymers in shear flow

The effects of EV and HI on the orientational properties of ring polymers is gained by the orientation resistance parameter m_G, which is defined as[28, 53]

$$m_G = \tan(2\theta)Wi = \frac{2G_{xy}}{G_{xx} - G_{yy}}Wi \qquad (9)$$

where θ is the angle between the projection of principal vector onto the flow-gradient plane and the flow direction (Fig.1).

The dependence of m_G on EV and HI as a function of Wi is shown in Fig.6. At small Wi ($Wi < 1$), G_{xx} is proportional to Wi and $G_{yy} - G_{zz}$ is proportional to Wi^2. Therefore, m_G is independent of Wi. In this region, the ring chains are close to their equilibrium conformations and only align along the flow direction. With Wi increasing, ring polymers orient with the flow direction and the conformations are strongly deformed. As shown in Fig.6, the values of the orientation resistance parameter m_G with EV are larger than the cases without EV. The reason is that the EV interaction leads to a weakening alignment of the ring polymers in the flow direction, consistent with the results for linear polymers[15, 20]. The curves in the presence of EV progressively approach a universal function, which increase as $m_G \sim Wi^{0.60}$ over the considered Wi range ($Wi > 20$). However, the orientation in the absence of EV follows the relationship $m_G \sim Wi^{0.56}$. Interestingly, the scaling exponent 0.56 is close to the exponent 0.54 reported for linear polymers with TB motion alone[52, 56]. The scaling exponents reflect that the probability for ring polymers without EV to take TT motions is quite low, because the ring polymer assumes a constant inclination angle with small fluctuations in TT motion[27-30]. Moreover, a universal curve is obtained for orientation with and without HI, implying that the orientation behaviors scaled with Wi have no qualitative difference in the presence and absence of HI[32].

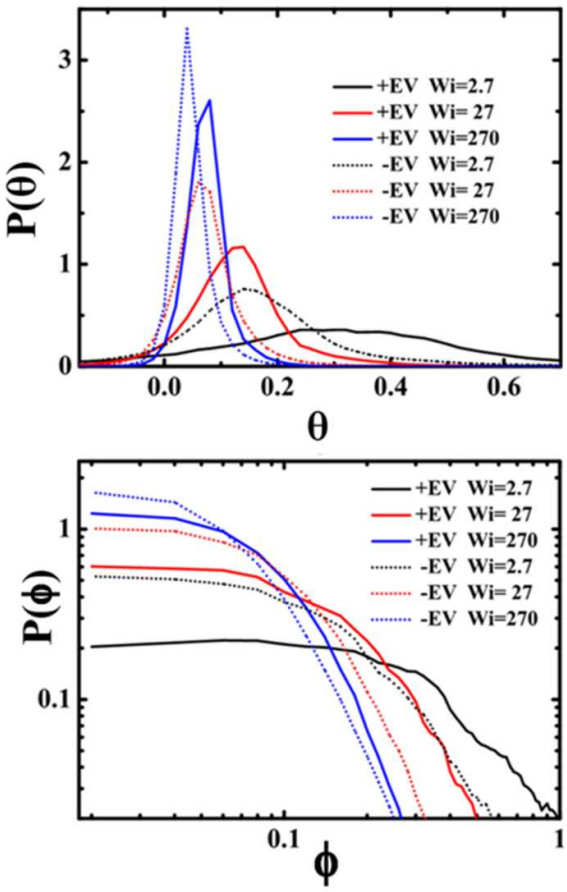

FIG. 7. Probability distribution functions $P(\theta)$ and $P(\phi)$ for ring polymers with and without EV interactions in logarithmic coordinates.

Further insight into the effects of EV and HI on the orientational behavior of ring polymers, the probability distribution functions (PDFs) $P(\theta)$ and $P(\phi)$ are calculated, where ϕ is the angle between the principal vector and its projection onto the flow-gradient plane, as shown in Fig.1. At equilibrium, no angle is preferred, and hence both $P(\theta)$ and $P(\phi)$ are uniform PDFs. When exposed to shear flow, the statistical conformation deviates from spherical symmetry and both $P(\theta)$ and $P(\phi)$ from uniform distribution. The results for probability distribution functions $P(\theta)$ with and without EV are displayed in Fig.7. Theoretical[57, 58], experimental[59], and numerical[60] studies for linear polymers show a crossover from a Gaussian shape of the distribution function to a power-law decay with shear strength increasing, $P(\theta) \sim (\sin\theta)^{-2}$, which is reproduced by our simulation for ring polymers. For a given Wi, $P(\theta)$ yields a wider distribution and a larger orientation angle under the effects of EV. Similar to $P(\theta)$, $P(\phi)$ also exhibits a significant shear dependence, as shown in Fig.7. The peak of the PDF shifts to smaller values with increasing Wi, and, at the same time, the width of $P(\phi)$ decreases. At high Wi, the PDF of angle ϕ can be described by a power law $P(\phi) \sim \phi^{-2}$, which is in accord with the depiction for linear polymers[60]. Moreover, in the presence of EV, $P(\phi)$ yields a slightly wider distribution at the same Wi.

D.Motion of ring polymers in shear flow

Individual ring polymers exhibit two primary types of motions, end-to-end TB like linear polymers and TT like fluid droplets and capsules[27]. In TB motion, ring chains continually undergo stretching, aligning, flipping, and collapsing with large deformation, while, in TT motion, the chain adopts an elliptical shape in the flow-gradient plane due to the strong EV interactions between the two strands of flexible ring polymers.

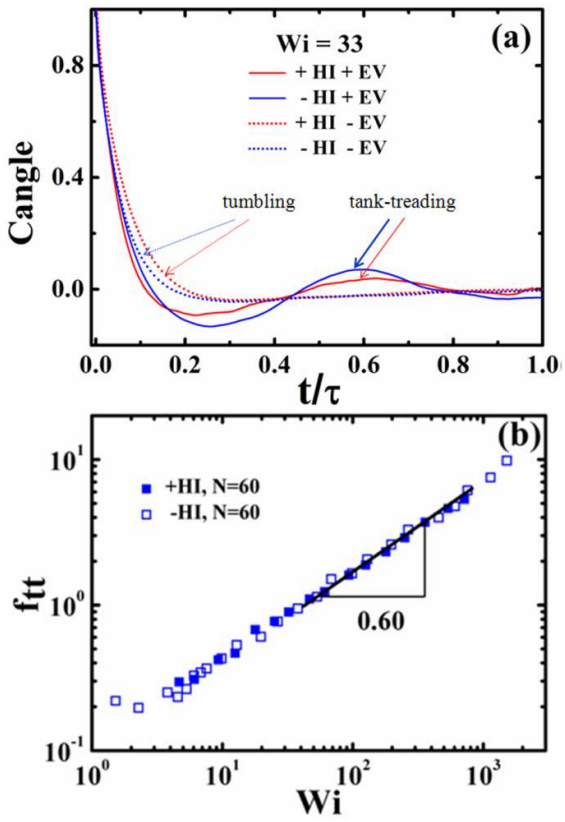

FIG. 8. (a) Angle autocorrelation functions C_{angle} for Wi = 33 with and without EV and HI. (b) Scaled tank-treading frequency f_{tt} with and without HI as a function of the Weissenberg number Wi. The solid line indicates the dependency $f_{tt} \sim Wi^{0.60}$.

In order to identify TT motion, the angular autocorrelation function $C_{\text{angle}}(t)$ is characterized quantitatively[27]. Similar to the linear polymers, the curves decay to zero sharply and no secondary peak is found in the absence of EV for ring polymers [see Fig.8(a)]. Ring polymers without EV However, the curves with EV interaction exhibit multiple peaks beside the first peak at t = 0, and they decay to zero at large time lags. Obviously, a ring polymer tends to form a two-strand line rather than an ellipse shape in the flow-gradient plane due to the lack of self-avoidance, and the TT motion is nearly

negligible. In addition, there is no obvious difference for the scaling behaviors of TT dynamics with and without HI. Moreover, the characteristic TT time τ_{tt} is defined as twice the secondary peak time, in which beads on chain can undergo one complete TT motion. The scaled TT frequency $f_{tt}=\tau/\tau_{tt}$, with the TT time scaled by the relaxation time τ, are presented in Fig.8(b). Remarkably, we find that the scaled frequency curves for the models with and without HI collapse onto a universal scaling function. Within the considered range of Wi ($Wi > 20$), dependence $f_{tt} \sim Wi^{0.60}$ is obtained.

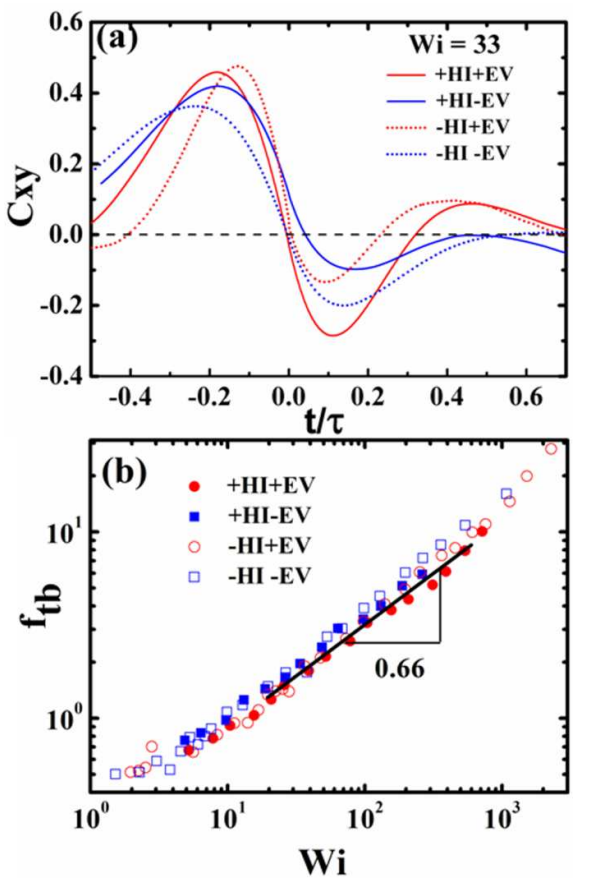

FIG. 9. (a) Cross-correlation functions C_{xy} for Wi = 33 in the presence and absence of EV and HI. (b) Scaled tumbling frequency f_{tb} as a function of the Weissenberg number Wi as indicated. The solid line indicates the dependency $f_{tb} \sim Wi^{0.66}$.

TB motion is determined by the cross-correlation function C_{xy} between the conformational changes in flow and gradient directions[33, 61]. Fig.9(a) shows C_{xy} in the presence and absence of EV and HI for Wi = 33. Similar to linear polymers, the curves of C_{xy} decay to zero at large time-lags, which implies that the TB motion of ring polymers is not perfect periodic. There are no quantitatively different with and without EV and HI at the same Wi. Furthermore, the curve of C_{xy} has a deep minimum at time $t_+ > 0$ and a pronounced peak at time $t_- < 0$. The characteristic time of the TB motion is defined as $\tau_{tb} = 2(t_+ - t_-)$ extracted from the correlation functions, corresponds to the shortest characteristic time for the collapse-stretching transition of chain conformation[61]. It has been shown for linear polymers that the characteristic frequency f_{tb} is depicted as a function of Wi with the power-law dependence $f_{tb} \sim Wi^{2/3}$ for $Wi >> 1$. Fig.9(b) shows the scaled TB frequency $f_{tb}=\tau/\tau_{tb}$ for ring polymers as a function of Wi. The data collapse onto a universal curve with the dependence $f_{tb} \sim Wi^{0.66}$ for large Wi. These results are consistent with those of linear polymers[33, 61]. It implies that normalized with Wi, the scaling behaviors of TB dynamics for ring polymers have no obvious difference in the presence or absence EV and HI.

Conclusions

A hybrid MPCD-MD simulation is carried out to investigate the influence of excluded volume and hydrodynamic interaction on the deformation, orientation and motion of ring polymers in shear flow. The strong excluded volume interaction suppresses deformation and orientation in the relaxation of shear-induced strain. In the absence of excluded volume, the shape of a ring polymer assumes a two-strand linear conformation rather than an ellipse in the flow-gradient plane. In this condition, ring polymers continually undergo end-over-end tumbling motion like linear polymers and the tank-treading motion is nearly negligible. Ring polymers without excluded volume show the seemingly universal behaviors with linear polymers despite the presence of hydrodynamic interaction in the scaling relationship for the deformation, orientation and tumbling motion. Hydrodynamic interaction can only change the scaling of relaxation time against polymer chain length, consistent with Zimm model prediction, but all other aspects scaled with Wi are almost unaffected. These findings that both topology and excluded volume are critical to maintain the deformation, orientation and motion of ring polymers in shear flow should be helpful to understand the behaviors of biomacromolecules with ring structure.

Acknowledgements

The work was supported by National Natural Science Foundation of China (21274153, 21334007, 21374117 and 21404105) and One Hundred Person Project of the Chinese Academy of Sciences. We are grateful to Computing Center of Jilin Province for essential support.

Notes and references

1. M. Rubinstein and R. H. Colby, *Polymer Physics*, Oxford University Press, Oxford, UK, 2003.
2. I. Teraoka, *Polymer Solutions: An Introduction to Physical Properties*, Polytechnic University, Brooklyn, New York, 2002.
3. A. Narros, C. N. Likos, A. J. Moreno and B. Capone, *Soft Matter*, 2014, **10**, 9601-9614.

4. J. A. Semlyen, *Cyclic Polymers*, Kluwer Academic Publishers, Dordrecht, 2001.
5. M. Trabi and D. J. Craik, *Trends Biochem. Sci.*, 2002, **27**, 132-138.
6. T. Sanchez, I. M. Kulic and Z. Dogic, *Phys. Rev. Lett.*, 2010, **104**, 098103.
7. C. Micheletti and E. Orlandini, *Macromolecules*, 2012, **45**, 2113-2121.
8. B. Alberts, A. Johnson, J. Lewis, M. Raff, K. Roberts and P. Walter, *Molecular Biology of the Cell*, Garland Science, New York, 2002.
9. K. A. Alamry, K. Nixon, R. Hindley, J. A. Odel and S. G. Yeates, *Macromol. Rapid. Comm.*, 2011, **32**, 316-320.
10. J. F. Sheng and K. F. Luo, *Phys. Rev. E*, 2012, **86**, 031803.
11. D. Michieletto, M. Baiesi, E. Orlandini and M. S. Turner, *Soft Matter*, 2015, **11**, 1100-1106.
12. E. Uliyanchenko, S. van der Wal and P. J. Schoenmakers, *Polym. Chem-Uk*, 2012, **3**, 2313-2335.
13. C. C. Huang, R. G. Winkler, G. Sutmann and G. Gompper, *Macromolecules*, 2010, **43**, 10107-10116.
14. E. C. Lee, M. J. Solomon and S. J. Muller, *Macromolecules*, 1997, **30**, 7313-7321.
15. A. Link and J. Springer, *Macromolecules*, 1993, **26**, 464-471.
16. J. G. H. Cifre and J. G. de la Torre, *Macromol. Theor. Simul.*, 2004, **13**, 273-279.
17. C. Sendner and R. R. Netz, *Eur. Phys. J. E*, 2009, **30**, 75-81.
18. K. D. Knudsen, J. G. de la Torre and A. Elgsaeter, *Polymer*, 1996, **37**, 1317-1322.
19. D. Petera and M. Muthukumar, *J. Chem. Phys.*, 1999, **111**, 7614-7623.
20. K. S. Kumar and J. R. Prakash, *J. Chem. Phys.*, 2004, **121**, 3886-3897.
21. E. C. Lee and S. J. Muller, *Polymer*, 1999, **40**, 2501-2510.
22. G. Witz, K. Rechendorff, J. Adamcik and G. Dietler, *Phys. Rev. Lett.*, 2011, **106**, 248301.
23. F. Drube, K. Alim, G. Witz, G. Dietler and E. Frey, *Nano. Lett.*, 2010, **10**, 1445-1449.
24. J. Suzuki, A. Takano and Y. Matsushita, *J. Chem. Phys.*, 2013, **139**, 184904.
25. T. Sakaue, *Phys. Rev. Lett.*, 2011, **106**, 167802.
26. Z. Benkova and P. Cifra, *Macromolecules*, 2012, **45**, 2597-2608.
27. W. D. Chen, J. Z. Chen and L. J. An, *Soft Matter*, 2013, **9**, 4312-4318.
28. W. D. Chen, J. Z. Chen, L. J. Liu, X. L. Xu and L. J. An, *Macromolecules*, 2013, **46**, 7542-7549.
29. W. Chen, Y. H. Zhao, L. Liu, J. Chen and L. An, *Polymer*, 2015, **64**, 93.
30. P. S. Lang, B. Obermayer and E. Frey, *Phys. Rev. E*, 2014, **89,** 022606.
31. C. M. Schroeder, E. S. G. Shaqfeh and S. Chu, *Macromolecules*, 2004, **37**, 9242-9256.
32. R. M. Jendrejack, J. J. de Pablo and M. D. Graham, *J. Chem. Phys.*, 2002, **116**, 7752-7759.
33. C. M. Schroeder, R. E. Teixeira, E. S. G. Shaqfeh and S. Chu, *Macromolecules*, 2005, **38**, 1967-1978.
34. R. Kapral, *Adv. Chem. Phys.*, 2008, **140**, 89-146.
35. M. Kroger, *Phys. Rep.*, 2004, **390**, 453-551.
36. A. Malevanets and R. Kapral, *J. Chem. Phys.*, 1999, **110**, 8605-8613.
37. A. Malevanets and R. Kapral, *J. Chem. Phys.*, 2000, **112**, 7260-7269.
38. A. Nikoubashman and C. N. Likos, *Macromolecules*, 2010, **43**, 1610-1620.
39. R. G. Winkler and C. C. Huang, *J. Chem. Phys.*, 2009, **130**, 074907.
40. M. K. Petersen, J. B. Lechman, S. J. Plimpton, G. S. Grest, P. J. in't Veld and P. R. Schunk, *J. Chem. Phys.*, 2010, **132**, 174106.
41. S. C. Ji, R. Jiang, R. G. Winkler and G. Gompper, *J. Chem. Phys.*, 2011, **135**, 104902.
42. B. Kowalik and R. G. Winkler, *J. Chem. Phys.*, 2013, **138**, 104903.
43. X. H. Wen, D. Zhang and L. X. Zhang, *Polymer*, 2012, **53**, 873-880.
44. M. P. Allen, and D. J. Tildesley, *Computer Simulation of Liquids*, Oxford University Press, New York, 1987.
45. M. Doi and S. F. Edwards, *The Theory of Polymer Dynamics*, Oxford University Press, New York, 1986.
46. M. Ripoll, K. Mussawisade, R. G. Winkler and G. Gompper, *Phys. Rev. E*, 2005, **72**, 016701.
47. T. Ihle, and D. M. Kroll, *Phys. Rev. E*, 2001, **63**, 020201.
48. G. Gompper, T. Ihle, D. M. Kroll and R. G. Winkler, *Advanced Computer Simulation Approaches for Soft Matter Sciences*, 2009, **221**, 1-87.
49. D. C. Rapaport, *The Art of Molecular Dynamics Simulation*, Cambridge University Press, New York, 2004.
50. S. Brown and G. Szamel, *J. Chem. Phys.*, 1998, **108**, 4705-4708.
51. C. Fu, W. Ouyang. Z. Sun and L. An, *J. Chem. Phys.*, 2007, **127**, 044903.
52. R. E. Teixeira, H. P. Babcock, E. S. G. Shaqfeh and S. Chu, *Macromolecules*, 2005, **38**, 581-592.
53. R. G. Winkler, *Phys. Rev. Lett.*, 2006, **97**, 128301.
54. R. G. Winkler, *J. Chem. Phys.*, 2010, **133**, 164905.
55. C. M. Schroeder, R. E. Teixeira. E. S. G. Shaqfeh and Steven Chu, *Macromolecules*, 2005, **38**, 1967-1978.
56. C. Aust, M. Kroger and S. Hess, *Macromolecules*, 1999, **32**, 5660-5672.
57. R. G. Winkler, *Phys. Rev. Lett.*, 2006, **97**, 128301.
58. M. Chertkov, I. Kolokolov, V. Lebedev and K. Turitsyn, *J. Fluid. Mech.*, 2005, **531**, 251–260.
59. S. Gerashchenko and V. Steinberg, *Phys. Rev. Lett.*, 2006, **96**, 038304.
60. A. Celani, A. Puliafito and K. Turitsyn, *EPL*, 2005, **70**, 464-470.
61. C. C. Huang, G. Sutmann, G. Gompper and R. G. Winkler, *EPL*, 2011, **93**, 54004.

highlights

In absence of excluded volume interaction, ring polymers show no significant difference to linear polymers, and tank-treading motion nearly negligible.

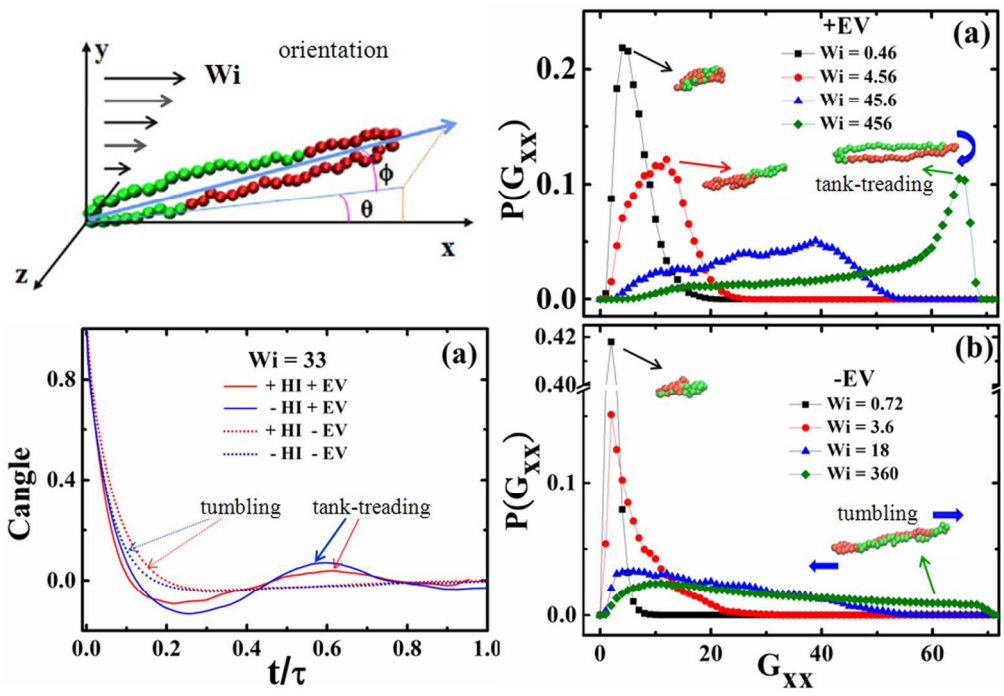

150x102mm (300 x 300 DPI)